# PET IMAGING OF DOSE DISTRIBUTION IN PROTON-BEAM CANCER THERAPY

by

**Joanne BEEBE-WANG, Avraham F. DILMANIAN, Stephen G. PEGGS, David J. SCHLYER, and Paul VASKA**

**Received on December 10, 2004; accepted on January 19, 2005**

**Proton therapy is a treatment modality of increasing utility in clinical radiation oncology mostly because its dose distribution conforms more tightly to the target volume than X-ray radiation therapy. One important feature of proton therapy is that it produces a small amount of positron-emitting isotopes along the beam-path through the non-elastic nuclear interaction of protons with target nuclei such as $^{12}$C, $^{14}$N, and $^{16}$O. These radioisotopes, mainly $^{11}$C, $^{13}$N, and $^{15}$O, allow imaging the therapy dose distribution using positron emission tomography. The resulting positron emission tomography images provide a powerful tool for quality assurance of the treatment, especially when treating inhomogeneous organs such as the lungs or the head-and-neck, where the calculation of the dose distribution for treatment planning is more difficult. This paper uses Monte Carlo simulations to predict the yield of positron emitters produced by a 250 MeV proton beam, and to simulate the productions of the image in a clinical PET scanner.**

*Key words: proton therapy, positron emission tomography, Monte Carlo simulation*

## INTRODUCTION

Positron emission tomography (PET) is potentially a very useful and powerful tool for monitoring of the distribution of the dose deposited in the patient from proton therapy [1–6]. This method is based on the detection of the positron-annihilation $\gamma$-rays following the decay of the small amounts of $\beta^+$ emitters (typically $^{11}$C, $^{13}$N, and $^{15}$O) produced via non-elastic nuclear reaction of protons with the target nuclei of the irradiated tissue. Verification of the therapy can be achieved by comparing the PET images discerning the $\beta^+$ activity distribution with the predicted target dose distribution used to plan the treatment.

The PET image is essentially the negative image of the target volume because the non-elastic nuclear reaction cross sections provide signal along most of the beam path, but diminish at the Bragg peak, where most of the proton energy is deposited via other interactions. However, an effective dose verification can still be made by comparing the radioisotope distribution measured by PET and the yield of the positron emitters predicted from the treatment planning code.

The possibility of proton therapy monitoring by means of PET was investigated by various groups [1–6]. However, due to the limitations of available non-elastic nuclear cross section data and detailed simulation codes, most of the simulation studies carried out in the past did not address the issue of the low energy end of the proton track, which is essential in monitoring the Bragg peak. In this paper, we examine the potential of PET as a quality assurance method for the full energy range (0.1-250 MeV) of the proton. The incentive for this work was the design of the Rapid Cycling Medical Synchrotron (RCMS) [7] at Brookhaven National Laboratory.

## POSITRON EMITTER PRODUCTION

During proton therapy, even though many isotopes are produced through different nuclear in-

Scientific paper
UDC: 621.039.38:616–006
BIBLID: 1451-3994, *20* (2005), 1, pp. 23-26

Authors' address:
Brookhaven National Laboratory
Upton, NY 11973, USA

E-mail address of corresponding author:
bbwang@bnl.gov (J. Beebe-Wang)

teractions, there are only 6 major channels producing the positron emitters $^{11}C$, $^{13}N$, and $^{15}O$ in human tissue. Table 1 summarizes these reactions. The cross sections shown in figs. 1 and 2 were extracted from the emission spectra of recoils in the data files provided by the ICRU Report 63 [8].

**Table 1. Relevant positron-emitter production reactions**

| Reaction | Threshold energy [MeV] | Half-life time [min] | Positron max. E [MeV] |
|---|---|---|---|
| $^{16}O$ (p, pn) $^{15}O$ | 16.79 | 2.037 | 1.72 |
| $^{16}O$ (p, 2p2n) $^{13}N$[a] | 5.66[c] | 9.965 | 1.19 |
| $^{14}N$ (p, pn) $^{13}N$ | 11.44 | 9.965 | 1.19 |
| $^{12}C$ (p, pn) $^{11}C$ | 20.61 | 20.39 | 0.96 |
| $^{14}N$ (p, 2p2n) $^{11}C$[a] | 3.22[c] | 20.39 | 0.96 |
| $^{16}O$ (p, 3p3n) $^{11}C$[b] | 27.50[c] | 20.39 | 0.96 |

[a] (p, 2p2n) is inclusive of (p, $\alpha$)
[b] (p, 3p3n) is inclusive of (p, $\alpha$pn)
[c] The listed thresholds refer to (p, $\alpha$) and (p, $\alpha$pn)

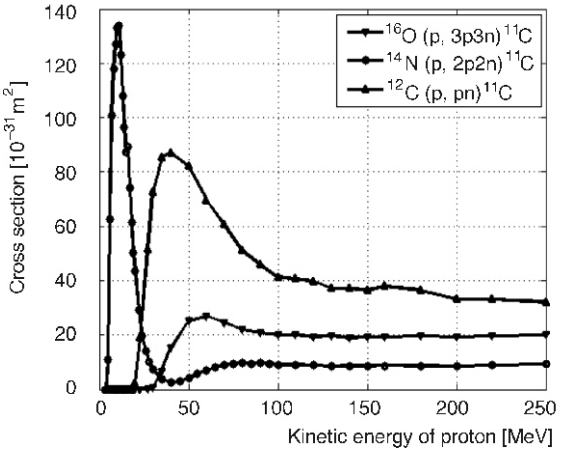


**Figure 1. Cross sections of nuclear reactions $^{16}O$ (p, 3p3n) $^{11}C$, $^{14}N$ (p, 2p2n) $^{11}C$, and $^{12}C$ (p, pn) $^{11}C$ *vs.* the kinetic energy of protons**

## MONTE CARLO SIMULATION

SRNA-BNL software package was used in this study. It was originally developed by R. D. Ilić (SRNA-2KG) [9], and was modified for this work to include also the production of positron emitter nuclei. SRNA-2KG is a Monte Carlo code for use in proton transport, radiotherapy, and dosimetry. Protons within an energy range of 100 keV to 250 MeV with pre-specified spectra are transported in a 3D geometry through material zones confined by planes and second order surfaces. SRNA-2KG can treat proton transport in 279 different kinds of materials including elements from Z = 1 to Z = 98 and 181 compounds and mixtures.

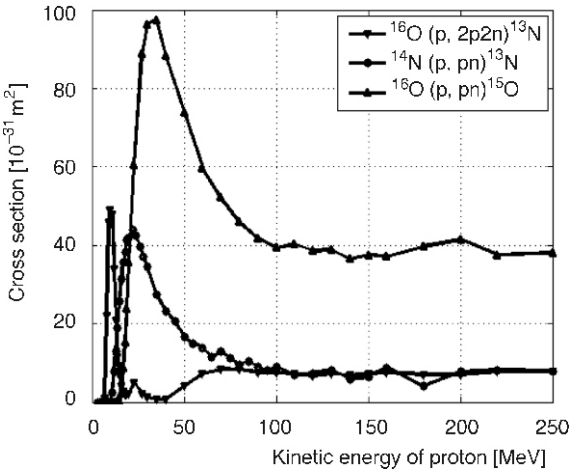


**Figure 2. Cross sections of nuclear reactions $^{16}O$ (p, 2p2n) $^{13}N$, $^{14}N$ (p, pn) $^{13}N$, and $^{16}O$ (p, pn) $^{15}O$ *vs.* the kinetic energy of protons**

The simulation of proton transport is based on the multiple scattering theory of charged particles and on a model for compound nucleus decay after proton absorption in non-elastic nuclear interactions. For each part of the range, an average loss of energy [10] is calculated with a fluctuation from Vavilov's distribution and with Schulek's correction [9]. The deflection angle of protons is sampled from Moliere's distribution [9]. SRNA-2KG has been benchmarked with the well know programs GEANT-3 [11] and PETRA [12]. Very good agreement was reached under the same conditions. Figure 3 shows the results comparison of a 250 MeV proton pencil beam in water phantom from SRNA-2KG and GEANT-3.

In SRNA-BNL software package, the positron emitters $^{11}C$, $^{13}N$, and $^{15}O$ are created through the decay processes of compound nuclei which include emission of protons, deuterons, tritons, alpha particles, or photons. The decay products are sampled using Poisson's distribution with appropriate average multiplication factors for each particle. Energy and angle of particle emissions, and the multiplication factors are obtained from comparing the direct cross sections available for reaching the daughter nuclei with that from the integration of differential cross sections [8] for non-elastic nuclear interactions. Energy and angle of secondary neutron emission are sampled from emission spectra. Transport of secondary protons follows that of primary protons of that particular energy. Spatial location and angle of neutron and photon are recorded, but not further treated. Emitted deuterons, tritons, and alpha particles are assumed to be absorbed at the location of their creation.

In order to assess the feasibility of effectively imaging the resulting positron emitter distribution, a realistic PET scan was then simulated using the SimSET Monte Carlo PET simulation package

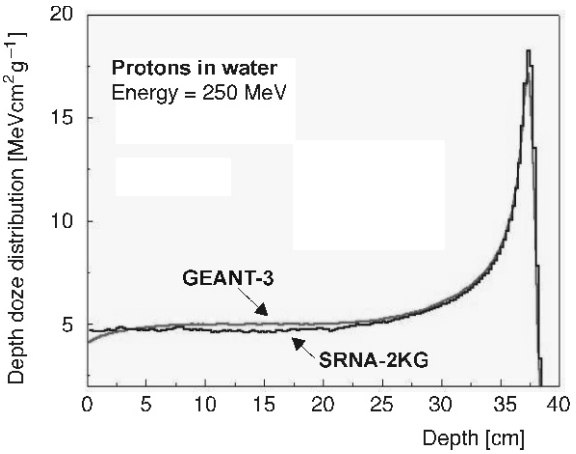


**Figure 3. Comparison of simulation results obtained from SRNA-2KG and GEANT-3 (Courtesy of Dr. R. D. Ilić)**

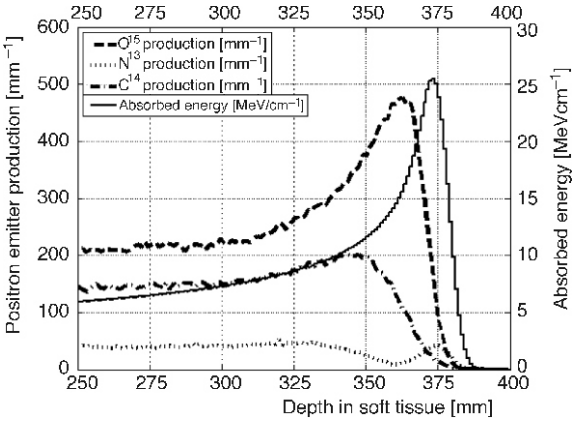


**Figure 4 The simulation results of linear production densities of $^{11}$C, $^{13}$N, and $^{15}$O *vs*. depth in soft tissue. The absorbed energy by the tissue is superimposed using a right-side vertical scale for depth comparison**

[13]. The software tracked each positron decay which occurred during a simulated 60-minute post-therapy scan. SimSET handles the most important aspects of the image formation process, including photon attenuation and scatter, geometry and photon acceptance of the tomograph, and binning of the coincidence data. The clinical whole-body Siemens/CTI HR+ tomograph was simulated with the proton beam direction aligned with the scanner axis. The binned projection data was reconstructed into volumetric images using the standard filtered back-projection technique.

## RESULTS

A 250 MeV proton beam with 2 mm diameter and a zero angle of divergence was transported in a human tissue using the SRNA-BNL simulation code. The soft tissue (ICRU 4-component) used in the simulation had a 0.55 ratio of the averaged atomic number to atomic mass (Z/A), and a density of 1.0 g/cm$^3$. The elemental composition of the tissue was 10.11% hydrogen, 11.11% carbon, 2.60% nitrogen, and 76.18% oxygen. The number of protons used in each set of the simulations was 4 $10^6$. This proton beam was estimated to produce an average absorbed dose of 2 Gy in the last 8.5 cm of its track, which is an appropriate estimate for treating a target volume 8.5 cm in diameter.

The positron emitter spatial distributions were simulated with the cross-sections shown in figs. 1 and 2. The results of linear production densities of $^{11}$C, $^{13}$N, and $^{15}$O are presented in fig. 4. In order to observe the details close to the Bragg peak, data were presented in the depth range of 250-400 mm. The linear production densities remain nearly constant at the depth under 250 mm due to the nearly constant values of the cross sections at proton energies above 100 MeV. In order to reduce the random noise, the values are obtained from averaging 225 sets of simulation data. The total energy absorbed by the tissue is superimposed with a right-side vertical scale in the same figure for depth comparison.

Figure 5 is a coronal slice from the reconstructed PET image. Despite less than 3000 coincidence counts in the entire image, the narrow trans-axial distribution and lack of background activity gives sufficient contrast to provide a reasonable definition of the distribution. The depth distribution of induced activity as determined from PET image is plotted in fig. 6.

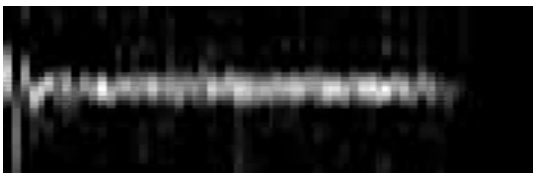

**Figure 5. A 0.8 mm slice through the activity distribution of the 3-dimentional PET image. The beam entered from the left. Horizontal (axial) dimension is 15 cm (full scanner FOV) and pixel size is 2.4 0.8 mm$^2$**

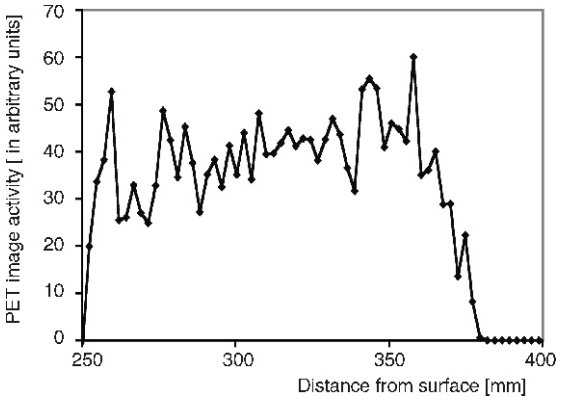


**Figure 6. Depth distribution of induced activity as determined from PET image**

## DISCUSSION AND CONCLUSION

The simulations demonstrate that, for 250 MeV protons and a typical radiotherapy dose of 2 Gy to the target volume during a therapy session, a subsequently acquired PET image will have sufficient signal-to-noise ratio to determine the depth profile of the induced activity distribution. Further work will be necessary. The ultimate goal is the verification of the measured PET image with a simulated PET image. Matching of these two images implies that the treatment was according to the plan. For treatment involving multiple ports including some opposing angles, in addition to the above effect, the centroid of the target dose can be computed with that of the PET image.

## ACKNOWLEDGEMENT

The authors would like to thank Dr. R. D. Ilić and the Imaging Research Laboratory at University Washington for providing SRNA-2KG and SimSET software packages. We also appreciate invaluable discussions with Drs. J. Liang, C. Woody, and J. S. Kovach.

This research was supported by the Laboratory Directed Research and Development (LDRD) program of Brookhaven National Laboratory, funded by the U. S. Department of Energy.

## REFERENCES

[1] Enghardt, W., Debus, J., Haberer, T., Hasch, B. G., Hinz, R., Jäkel, O., Krämer, M., Lauckner, K., Pawelke, J., Pönisch, F., Positron Emission Tomography for Quality Assurance of Cancer Therapy with Light Ion Beams, *Nucl. Phys., A 654* (1999), 1, Supplement 1, pp. 1047c-1050c

[2] Parodi, K., Enghardt, W., Potential Application of PET in Quality Assurance of Proton Therapy, *Phys. Med. Biol., 45* (2000), 11, pp. N151-N156

[3] Fassò, A., Ferrari, A., Sala, P. R., Electron-Photon Transport in FLUKA: Status, *Proceedings*, Monte Carlo 2000, Lisbon, Portugal, October 23-26, 2000, pp. 159-164

[4] Oelfke, U., Lam, G. K. Y., Atkins, M. S., Proton Dose Monitoring with PET: Quantitative Studies in Lucite, *Phys. Med. Biol., 41* (1996), 1, pp. 177-196

[5] Parodi, K., Enghardt, W., Haberer, T., In-Beam PET Measurements of $\beta^+$ Radioactivity Induced by Proton Beams, *Phys. Med. Biol., 47* (2002), 1, pp. 21-26

[6] Paans, A. M. J., Schippers, J. M., Proton Therapy in Combination with PET as Monitor: A Feasibility Study, *IEEE Trans. Nucl. Science, 40* (1993), 4, pp. 1041-1043

[7] Peggs, S., Barton, D., Beebe-Wang, J., *et al*., The Rapid Cycling Medical Synchrotron, RCMS, *Proceedings*, 8th European Particle Accelerator Conference (EPAC-2002), Paris, June 3-7, 2002, pp. 2754-2756

[8] ***, ICRU Report 63, Nuclear Data for Neutron and Proton Radiotherapy and for Radiation Protection, MD, USA, 2000

[9] Ilić, R. D., Lalić, D., Stanković, S. J., SRNA – Monte Carlo Codes for Proton Transport Simulation in Combined and Voxelized Geometries, *Nuclear Technology & Radiation Protection*, *17* (2002), 1-2, pp. 27-36

[10] ***, ICRU Report 49, Stopping Power and Ranges for Protons and Alpha Particles, MD, USA 1993

[11] ***, GEANT 1994 CERN Program Library Long Writeup W5013, 1994

[12] Medin, J., Studies of Clinical Proton Dosimetry Using Monte Carlo Simulation and Experimental Techniques, Ph. D. thesis, Stockholm Univ., 1997

[13] Harrison, R. L., Vannot, S. D., Kaplan, M. S., Lewellen, T. K., Slat Collimation and Cylindrical Detectors for PET Simulations Using SimSET, IEEE Nuclear Science Symposium, 2000, Conference Record, vol. 3, pp. 20/89-20/92

---

**Џоана БИБИ-ВАНГ, Абрахам Ф. ДИЛМАНИАН,
Стефан Г. ПЕГС, Давид Ј. ШЛАЈЕР, Паул ВАСКА**

## PET ВИЗУЕЛИЗАЦИЈА РАСПОДЕЛЕ ДОЗЕ У ЛЕЧЕЊУ РАКА ПРОТОНСКИМ СНОПОМ

У клиничкој радијационој онкологији све више се користи лечење протонима, пре свега што се расподела дозе много боље слаже са запремином мете него при лечењу Х-зрачењем. Једна значајна особина протонске терапије је да нееластичним нуклеарним интеракцијама протона са језгрима мете, на пример, $^{12}C$, $^{14}N$ и $^{16}O$, дуж пута снопа настају мале количине изотопа који емитују позитроне. Ови радиоизотопи, углавном $^{11}C$, $^{13}N$ и $^{15}O$, омогућавају визуелизацију расподеле терапијске дозе коришћењем позитронске емисионе томографије – PET. Образована PET визуелизација представља моћно средство за осигурање квалитета поступка, посебно када се лече нехомогени органи, плућа или глава са делом врата, када је прорачун расподеле дозе у планирању лечења веома тежак. У раду се користи Монте Карло симулација ради процене приноса позитронских емитера произведених протонским снопом енергије 250 MeV, као и ради предвиђања образовања слике на клиничком PET скенеру.

*Кључне речи: лечење протонима, позитронска емисиона томографија, Монте Карло симулација*